

Updated Recommendations for Modifications to the AEDT for Improved Noise Modeling of Advanced Air Mobility Vehicles

Stefan J. Letica
Langley Research Center, Hampton, Virginia

Stephen A. Rizzi
Langley Research Center, Hampton, Virginia

NASA STI Program Report Series

Since its founding, NASA has been dedicated to the advancement of aeronautics and space science. The NASA scientific and technical information (STI) program plays a key part in helping NASA maintain this important role.

The NASA STI Program operates under the auspices of the Agency Chief Information Officer. It collects, organizes, provides for archiving, and disseminates NASA's STI. The NASA STI Program provides access to the NTRS Registered and its public interface, the NASA Technical Report Server, thus providing one of the largest collections of aeronautical and space science STI in the world. Results are published in both non-NASA channels and by NASA in the NASA STI Report Series, which includes the following report types:

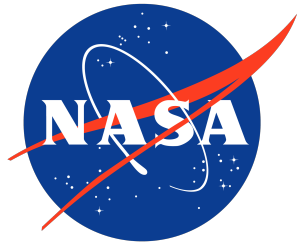
- **TECHNICAL PUBLICATION.** Reports of completed research or a major significant phase of research that present the results of NASA programs and include extensive data or theoretical analysis. Includes compilations of significant scientific and technical data and information deemed to be of continuing reference value. NASA counterpart of peer-reviewed formal professional papers, but having less stringent limitations on manuscript length and extent of graphic presentations.
- **TECHNICAL MEMORANDUM.** Scientific and technical findings that are preliminary or of specialized interest, e.g., quick release reports, working papers, and bibliographies that contain minimal annotation. Does not contain extensive analysis.
- **CONTRACTOR REPORT.** Scientific and technical findings by NASA-sponsored contractors and grantees.

- **CONFERENCE PUBLICATION.** Collected papers from scientific and technical conferences, symposia, seminars, or other meetings sponsored or co-sponsored by NASA.
- **SPECIAL PUBLICATION.** Scientific, technical, or historical information from NASA programs, projects, and missions, often concerned with subjects having substantial public interest.
- **TECHNICAL TRANSLATION.** English-language translations of foreign scientific and technical material pertinent to NASA's mission.

Specialized services also include organizing and publishing research results, distributing specialized research announcements and feeds, providing information desk and personal search support, and enabling data exchange services.

For more information about the NASA STI Program, see the following:

- Access the NASA STI program home page at <http://www.sti.nasa.gov>
- Help desk contact information: <https://www.sti.nasa.gov/sti-contact-form/> and select the "General" help request type.



Updated Recommendations for Modifications to the AEDT for Improved Noise Modeling of Advanced Air Mobility Vehicles

Stefan J. Letica
Langley Research Center, Hampton, Virginia

Stephen A. Rizzi
Langley Research Center, Hampton, Virginia

National Aeronautics and
Space Administration

Langley Research Center
Hampton, Virginia 23681-2199

September 2025

Acknowledgments

The authors acknowledge many helpful discussions with Kevin Shepherd, Andrew Christian, and Doug Boyd of NASA's Langley Research Center, with Bradley Nicholas, Eric Boeker, and Steve Goetzinger of the U.S. DOT Volpe National Transportation Systems Center, and with David Senzig, Fabio Grandi, and Joseph DiPardo of the FAA Office of Environment and Energy.

<p>The use of trademarks or names of manufacturers in this report is for accurate reporting and does not constitute an official endorsement, either expressed or implied, of such products or manufacturers by the National Aeronautics and Space Administration.</p>

Available from:

NASA STI Program / Mail Stop 150
NASA Langley Research Center
Hampton, VA 23681-2199

Abstract

Urban Air Mobility (UAM) vehicles are an up-and-coming technology in the realm of commercial aviation. As with any other flying vehicle operating in the vicinity of people, how the noise these vehicles create impacts local communities must be investigated and understood. The Federal Aviation Administration (FAA) Aviation Environmental Design Tool (AEDT) is the required tool for performing noise and emissions studies for compliance with the National Environmental Policy Act (NEPA). This tool allows the modeling of fixed-wing and helicopter vehicles, but it does not specifically support UAM vehicle modes. This TM documents the final set of recommendations to the FAA from NASA's Revolutionary Vertical Lift Technology (RVLT) project for improving the AEDT for modeling UAM vehicles using either of the pre-existing fixed-wing or helicopter modes.

Contents

1	Background	6
1.1	Document Overview	6
1.2	Previously Published Work	7
2	Prior Observations	8
2.1	Fixed-Wing Modeling	8
2.2	Helicopter Modeling	8
2.3	Common to Fixed-Wing and Helicopter Modeling	9
3	Flight Operation Observations	9
3.1	Overflight	9
3.1.1	A Brief Note on the Duration Adjustment	10
3.1.2	Comparison of AEDT and Simulation Analyses for Overflight	12
3.2	Approach	15
3.2.1	Comparison of AEDT and Simulation Analyses for Approach	22
3.3	Departure	24
3.3.1	Comparison of AEDT and Simulation Analyses for Departure	27
4	Recommendations	30
4.1	Fixed-Wing Modeling	31
4.1.1	Prior Recommendations	31
4.1.2	New Recommendations	32
4.2	Helicopter Modeling	32
4.2.1	Prior Recommendations	32
4.2.2	New Recommendations	33
4.3	Other	33
4.3.1	Prior Recommendations	33
4.3.2	New Recommendations	34

Nomenclature

Δ_{trk}	= Delta distance for ground track, ft
ϕ	= azimuth (sideline) angle, deg
θ	= polar angle, deg
D	= Distance along track from approach/departure end of runway, ft
DIR	= Ground-based directivity at start of takeoff roll
d_{-1}	= Coordinate value of profile point immediately before touchdown point, ft
D_{app}	= Displaced approach threshold, ft
D_{dep}	= Displaced departure threshold, ft
E	= total sound exposure, Pa ² -s
h_{tc}	= Runway threshold crossing height, ft
L	= sound pressure level, dB
L_{EPN}	= Effective perceived noise level, dB
L_E	= sound exposure level, dB
L_{PNT}	= Tone-corrected perceived noise level, dB
LD	= Lateral directivity
V	= Speed, kt
z_{-1}	= Altitude AFE of profile point immediately before touchdown point, ft

Subscripts

A	= A-weighted
ADJ	= adjustment
mx	= maximum level
0	= reference value

List of Figures

1	L_{AE} for fixed-wing mode in straight and level overflight.	11
2	L_{AE} for helicopter mode in straight and level overflight with lateral directivity.	11
3	Directivity angle definitions (ϕ : lateral/azimuthal angle, θ : polar angle).	12
4	Difference between L_{AE} for fixed-wing and helicopter modes when including lateral directivity.	13
5	Difference between L_{AE} for fixed-wing and helicopter modes when using axisymmetric helicopter NPD data.	13
6	Comparison of AEDT (filled) and AMAT (lines) generated L_{AE} for fixed-wing mode in straight and level overflight.	14
7	Comparison of AEDT (filled) and AMAT (lines) generated L_{AE} for helicopter mode in straight and level overflight.	14
8	Bell 206L Long Ranger standard approach profile used as a basis for the UAM vehicle approach.	15
9	Profile for the AEDT approach analyses. The heavy black horizontal line shows the extent of a one-mile runway with the landing point at the left (west) end. The landing point is located at $(x, y) = 0, 0$ ft, with positive x to the right (east).	16
10	L_{AE} for fixed-wing mode on approach.	19
11	L_{AE} for helicopter mode on approach with lateral directivity.	19
12	L_{AE} for fixed-wing mode on approach using 2 NPD curves.	20
13	L_{AE} for helicopter mode on approach without lateral directivity.	20
14	Difference between baseline approach analyses (Figure 10 and Figure 11). Positive difference indicates that the fixed-wing analysis predicts higher noise exposure than the helicopter analysis at that location.	21
15	Difference between modified approach analyses (Figure 12 and Figure 13). Positive difference indicates that the fixed-wing analysis predicts higher noise exposure than the helicopter analysis at that location.	21
16	AEDT (filled) and AMAT (lines) L_{AE} contours for fixed-wing mode on approach (full view).	22
17	AEDT (filled) and AMAT (lines) L_{AE} contours for fixed-wing mode on approach (close-up view).	22
18	AEDT (filled) and AMAT (lines) L_{AE} contours for helicopter mode on approach (full view).	23
19	AEDT (filled) and AMAT (lines) L_{AE} contours for helicopter mode on approach (close-up view).	23
20	Bell 206L Long Ranger standard departure profile used as a basis for the UAM vehicle departure.	24
21	Profile for the AEDT departure analyses. The heavy black horizontal line shows the extent of a one-mile runway with the takeoff point at the right (east) end. The takeoff point is located at $(x, y) = 0, 0$ ft, with positive x to the right (east).	25
22	L_{AE} for fixed-wing mode on departure.	27

23	L_{AE} for helicopter mode on departure with lateral directivity.	27
24	L_{AE} for fixed-wing mode on departure using 2 NPD curves.	28
25	L_{AE} for helicopter mode on departure without lateral directivity. . .	28
26	Difference between baseline departure analyses (Figure 22 and Figure 23). Positive difference indicates that the fixed-wing analysis predicts higher noise exposure than the helicopter analysis at that location. .	29
27	Difference between baseline departure analyses (Figure 24 and Figure 25). Positive difference indicates that the fixed-wing analysis predicts higher noise exposure than the helicopter analysis at that location. .	29
28	AEDT (filled) and AMAT (lines) generated L_{AE} for fixed-wing mode on departure (full view).	30
29	AEDT (filled) and AMAT (lines) generated L_{AE} for fixed-wing mode on departure (close-up view).	30
30	AEDT (filled) and AMAT (lines) generated L_{AE} for helicopter mode on departure (full view).	31
31	AEDT (filled) and AMAT (lines) generated L_{AE} for helicopter mode on departure (close-up view).	31

1 Background

The following is an updated set of observations and recommendations for modifications to the FAA Aviation Environmental Design Tool (AEDT) [1] version 3g based on focused studies in modeling noise of Advanced Air Mobility (AAM) vehicle noise, particularly the subset of Urban Air Mobility (UAM) vehicles, using both fixed-wing and helicopter modes within the AEDT. This document contains both a preliminary set of recommendations and an updated set. The preliminary set was provided to the FAA Office of Environment and Energy in February 2023 via informal communication, and the analyses in that document were performed using the AEDT version 3e. The updated set includes data that are intended to support the recommendations. As with the preliminary set of recommendations, a separate set of recommendations is offered for each modeling approach (fixed-wing and helicopter modes) without specifying a preferred approach. All AEDT analyses in this document were performed using the AEDT version 3g, and likewise, all recommendations are made with reference to version 3g. At the time of writing, the release of the AEDT version 4a is imminent and will incorporate some of the recommendations contained in this document. Addressing these, however, is outside the scope of this document, so the authors will refrain from commenting on version 4a further.

1.1 Document Overview

This document is organized as follows: Section 2 reiterates the prior set of observations not specific to the flight operation types (overflight, departure, and approach). Section 3 offers a set of observations for fixed-wing and helicopter modes that is particular to three flight operation types. Section 4 offers the updated set of recommendations based on Sections 2 and 3.

In the following, all AEDT analyses were performed using noise-power-distance (NPD) data generated from predictions [2] of the NASA quadrotor reference vehicle [3]. For the fixed-wing analyses, the reference vehicle was considered to be a propeller-driven aircraft configuration and fixed-point flight profiles were used. All analyses were run with terrain turned off, i.e., flat earth.

In addition to comparisons between the AEDT analyses, comparisons of AEDT analyses with simulation data generated using the NASA Aircraft Noise Prediction Program 2 (ANOPP2) [4] Mission Analysis Tool (AMAT) are provided. The AMAT is a time-marching simulation program that uses the full source noise hemisphere, akin to the Volpe Advanced Acoustic Model (AAM) [5]. The AMAT is being used in order to i) use the full source noise directivity (which neither the AEDT fixed-wing nor helicopter analyses incorporate) and ii) use as many source noise hemispheres as are needed for the particular operation without restriction (something that the AEDT fixed-wing fixed-point profiles allow but that helicopter mode does not, see Section 3.2). Noting that there are differences between AMAT propagation algorithms and other AEDT adjustments (e.g., lateral attenuation adjustment), the AMAT analyses are used as a means of examining the effect of removing the directivity and sequencing restrictions in the AEDT. Though it does incorporate physics

more directly into the final result, the authors are not suggesting that it is the “truth.”

1.2 Previously Published Work

The authors published a number of relevant works following the preliminary recommendations made in February 2023:

- In Ref. [6], the authors developed a method for evaluating UAM vehicle community noise using the AEDT in helicopter mode, as well as evaluation using hybrids of helicopter mode and fixed-wing mode. This was done by casting fixed-wing flight segments to appropriate helicopter operational mode analogues. It was shown that in the areas with the highest sound exposure levels, i.e. takeoff and landing areas, there were significant differences between helicopter and fixed-wing modes. It was noted in this work that compromises had to be made for modeling UAM operations in helicopter mode, as the AEDT $\leq 3g$ (versions of the AEDT before and including 3g) have several restrictions on the helicopter operational modes that are allowed and on their sequence. These are tabulated in Ref. [1]. It was also noted that one weakness of the hybrid approach was that NPD data for both fixed-wing and helicopter modes must be provided, rendering it impractical for all but investigative studies.
- In Ref. [7], a subsequent investigation was conducted to find the source of differences between otherwise equivalent AEDT fixed-wing and helicopter mode operations in takeoff and landing areas using simplified flight profiles. The simplified flight profiles were based on the Bell 206 standard departure and approach profiles. Operations were run in the AEDT using the NASA RVLTL quadrotor. This study showed very large differences between fixed-wing mode and helicopter mode in the vicinity of takeoff and landing areas. It was thought that these differences were primarily due to the noise fraction calculation. Additionally, comparisons were made to simulations emulating the AEDT operations using a NASA time-marching simulation tool (see Section 1.1). These comparisons showed that while helicopter mode provides better comparisons to the simulated contours on the sidelines, the inability to use multiple approach/departure NPD curves limited the capture of fine details in the contours, especially in the vicinity of takeoff and landing areas.
- To further understand the nature of the differences between fixed-wing mode and helicopter mode, a deeper dive into the noise fraction was conducted in Ref. [8]. The noise fraction calculation was derived and visualized. During this investigation, an incompatibility was discovered between the reference speed used for helicopter NPDs and the reference speed used for the noise fraction calculation. As implemented in the AEDT $\leq 3g$, the reference speed for the noise fraction calculation was hardwired to be 160 kt, but the helicopter NPD data provided at other reference speeds were not corrected to 160 kt for the calculation. This mismatch was shown to cause severe distortion of the noise contours, including those seen in Ref. [7]. Analyses put forth in this document

implement a workaround until such time as the AEDT implementation of the noise fraction adjustment is updated. The workaround corrects the noise exposure data for the helicopter to 160 kt from the original reference speed based on the duration adjustment (Section 3.1).

Some of the results from the above publications, as well as the results from studies performed in the current work, are the basis upon which the recommendations in this document are put forth.

2 Prior Observations

The set of observations made in the 2023 preliminary recommendations document are reproduced here for completeness. None have changed as a result of the analyses detailed in Section 3.

2.1 Fixed-Wing Modeling

- A generic performance model applicable to a wide range of AAM vehicle architectures is very unlikely. For example, VTOL-capable aircraft powered by non-tilting rotors differ in performance and noise characteristics from VTOL-capable aircraft powered by tilting rotors.
- Identification of a single variable correlating noise with operating condition for AAM vehicles, such as corrected net thrust, is very unlikely.
- The hover, vertical ascent, and vertical descent conditions can be modeled using a short, very low-speed flight segment. However, the noise contour shape is controlled by the noise fraction algorithm, which is inappropriate for this flight condition.
- The fixed-wing approach using fixed-point flight profiles is simple, intuitive, and robust. This allows complicated point-to-point flight trajectories to be modeled as a single operation.

Because of the above observations, modeling of AAM vehicle noise in fixed-wing mode is limited to using fixed-point flight profiles.

2.2 Helicopter Modeling

- The limited number of operational modes (e.g., a single approach or departure condition) and other restrictions (including those limiting the number and sequence of allowable operational procedural steps) inhibit the modeling of AAM vehicle operations.
- Related to the above, point-to-point operations require trajectories to be segmented into departure, overflight, and approach. Study setup is both time-consuming and error-prone, and it likely presents an obstacle to the typical AEDT user.

2.3 Common to Fixed-Wing and Helicopter Modeling

- In contrast to typical AEDT usage for developing noise contours around airports, in which some aircraft depart to some distant airport and other aircraft arrive from some other distant airport, AAM vehicles operate in a limited area, necessitating a robust capability for point-to-point operations.
- There are many different point-to-point operations that occur within the same study area, making the reference altitude for each operation ambiguous.
- There are “workarounds” such as modeling a point-to-point route entirely as a departure or an approach (fixed-wing) or as a departure/overflight/approach (helicopter), but doing so is cumbersome and error-prone.

Comments about the process being cumbersome were made in the context of the studies performed in Refs. [6] and [9]. This problem is somewhat mitigated by NASA’s development of MATLAB scripts for transforming NASA route and vehicle data into comma-separated value (CSV) files, which are then loaded via a set of Volpe-developed structured query language (SQL) scripts into the AEDT database. The MATLAB scripts are not available outside of NASA.

3 Flight Operation Observations

As stated previously, modeling a point-to-point operation in the AEDT in helicopter mode necessitates combining three operations. These operations – departure, overflight, and approach – must be placed into a single operations group, from which an annualization and analysis job can be created. This requires sectioning the full route into departure, overflight, and approach sections, as detailed in Ref. [6]. To enable direct comparisons of fixed-wing and helicopter mode in each operation type, individual studies of each operation type were performed. These are detailed in this section.

In all of the following analyses, the observers are defined at (x, y) points, where x is positive east and y is positive north. No terrain data are used (flat earth), and the AEDT default definition of receptor height (4 ft above ground) is used; these conditions are replicated in all AMAT analyses.

3.1 Overflight

The flight operation observations begin with an overflight operation, as it has the fewest differences between modeling aircraft in fixed-wing versus helicopter modes. The modeled flyover traverses from west to east over a single segment with an extended 20 mi flight path centered over a 3 mi x 3 mi receptor grid such that end-of-segment effects are well outside of the grid. Flight conditions are 90 kt with 0° climb angle at 1000 ft above field elevation (=0 ft MSL). The helicopter analyses were performed using mode L (level flyover) with the B coefficients (B_0 , B_1 , B_2) for the AEDT advancing tip Mach number adjustment (AEDT Technical Manual Eq.

4-59 [1]) set to zero, as it is unclear whether or not this adjustment is appropriate for AAM vehicles.

Helicopter data are normally provided to the AEDT with individual reference speeds specified for each operational mode. To eliminate the effect of the incorrect noise fraction adjustment [8], all helicopter sound exposure level NPD data were corrected to a reference speed of 160 kt.

AEDT-computed A-weighted SEL (L_{AE}) data are shown in Figure 1 and Figure 2 for the fixed-wing and helicopter mode analyses, respectively. As can be seen, exposure levels for receptors directly below the flight track compare favorably, while exposure levels for lateral receptors are lower for the helicopter due to the lateral directivity adjustment. The helicopter analysis includes NPD data at azimuth angles of $\phi = \pm 45^\circ$ that differ from data at $\phi = 0^\circ$ (directly below), see Figure 3. In other words, the lateral directivity adjustment for helicopters in the AEDT is behaving as intended. The difference is more clearly seen in Figure 4.

Note that Figure 2 is very symmetric about the ground track since the NPD data are nearly symmetric (see Ref. [2]).

The specific effect of including the AEDT helicopter lateral directivity adjustment can be ascertained by running a helicopter mode analysis and manually setting $\phi = \pm 45^\circ$ NPD data to be identical to the $\phi = 0^\circ$ data, that is, when using axisymmetric NPD data. The difference is then negligible, as shown in Figure 5.

Ref. [8] provides more details on the specific adjustments that are equalized and/or negated between helicopter and fixed-wing mode in order to produce the result in Figure 5. This shows that functionally identical helicopter and fixed-wing mode results can be achieved in overflight operations when the two are made as equal as possible within the AEDT inputs.

3.1.1 A Brief Note on the Duration Adjustment

The duration adjustment (AEDT Technical Manual Eq. 4-26 [1]) is given as:

$$DUR_{ADJ} = 10 \log_{10} \left[\frac{AS_{ref}}{AS_{seg}} \right] \quad (1)$$

in which AS_{ref} is the reference aircraft speed (160 kts for fixed-wing aircraft and various values for flyover, departure, and approach for helicopters), and AS_{seg} is the aircraft speed at the closest point of approach.

The AEDT Technical Manual points out that helicopters are referenced to different speeds (as noted above), but it does not point out that these are applied to the different operational mode procedural steps and not the operation type (overflight, departure, or approach). For example, an approach operation profile starts with a level flyover step (mode L) followed by a number of approach steps (modes A-C). Within the one approach operation, the level flight procedural steps use one AS_{ref} for their duration adjustment, while descending and/or decelerating procedural steps use a different AS_{ref} for their duration adjustment. Although confusing at first, the calculation is performed correctly within the AEDT; it just is not adequately documented.

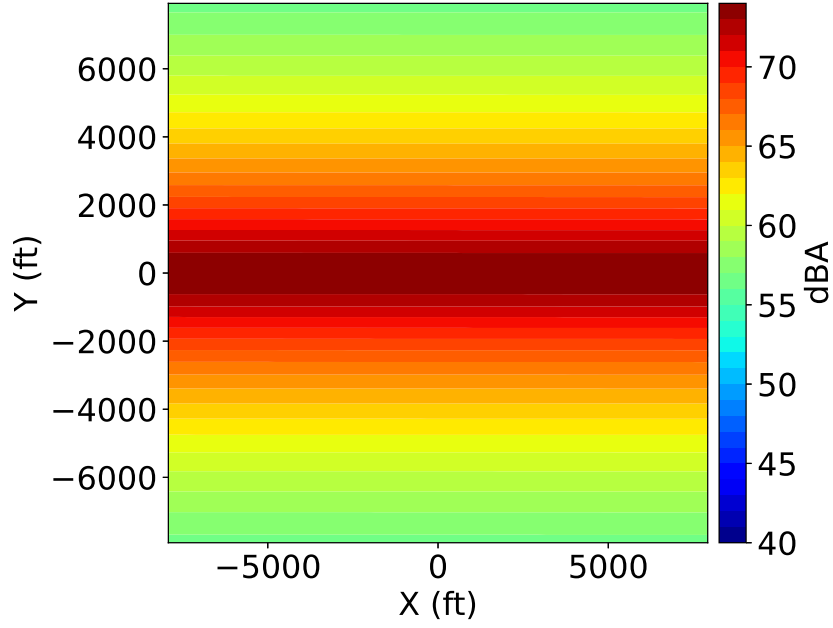


Figure 1: L_{AE} for fixed-wing mode in straight and level overflight.

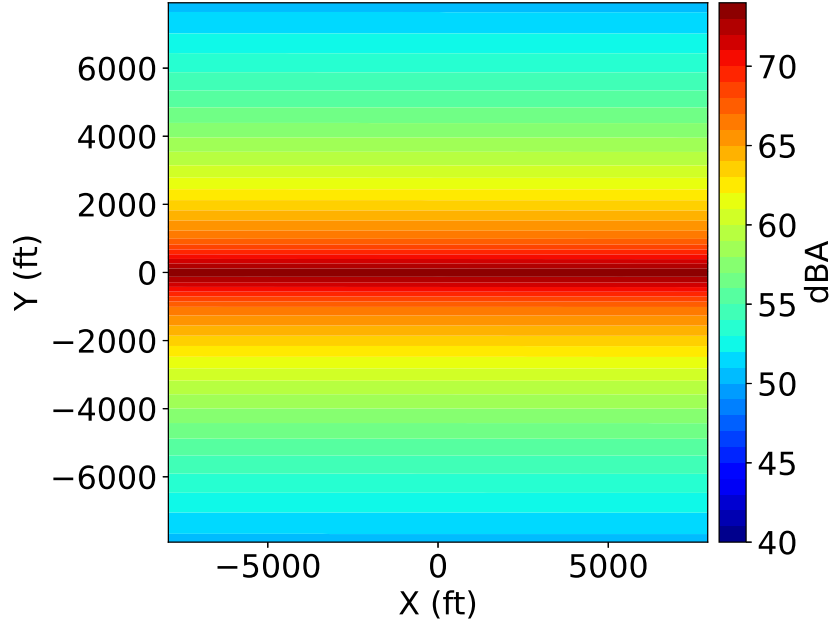


Figure 2: L_{AE} for helicopter mode in straight and level overflight with lateral directivity.

The implication of using a different AS_{ref} for different operational mode procedural steps is that if multiple operational mode procedure steps of the same type but different character (i.e., A_1 , A_2 , A_3) are allowed in some future version of the

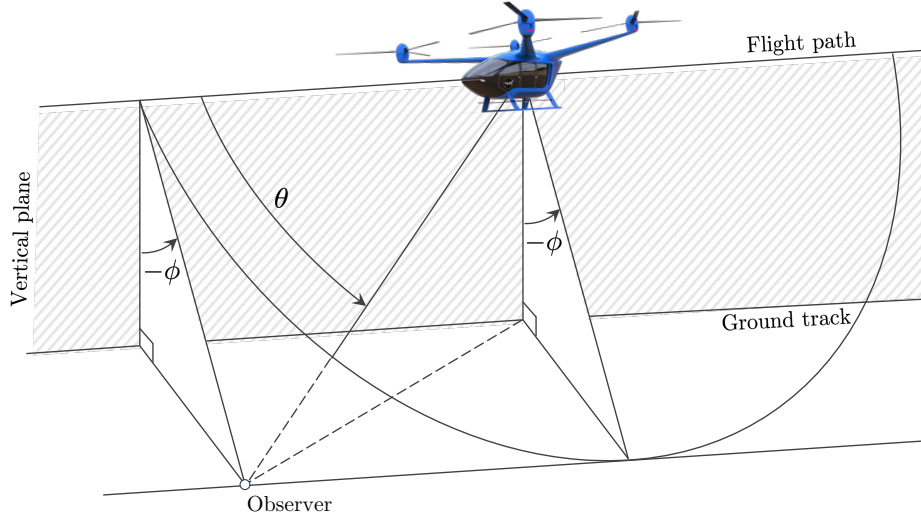


Figure 3: Directivity angle definitions (ϕ : lateral/azimuthal angle, θ : polar angle).

AEDT, each at a different speed (entirely possible for fixed-wing fixed-point flight profiles), then either:

- there will be a need to specify a different reference speed for each unique operational mode procedural step, or
- follow the fixed-wing process and adjust all helicopter NPD data to a single reference speed, e.g., 160 kt. This is likely the least ambiguous to the provider of helicopter mode NPD data.

3.1.2 Comparison of AEDT and Simulation Analyses for Overflight

Next, simulation data from the AMAT (using the full source directivity) are compared with AEDT analyses for fixed-wing and helicopter modes. The AEDT analyses from Figures 1 and 2 were repeated for a flight path from $x = -3$ mi to $x = 3$ mi, as in Ref. [8]. Notably, this allows for the inclusion of end-of-segment effects in the analysis. This analysis was repeated for an identical grid of ground receptors in the AMAT. Figure 6 and Figure 7 show the AEDT contours from Ref. [8], with the AMAT-produced contours overlaid.

In contrast to Figure 6, Figure 7 shows that the helicopter lateral directivity adjustment in the AEDT compares more favorably with the AMAT data within the $\phi = \pm 45^\circ$ azimuth range (for the 1000 ft overflight, this is bounded by $y = \pm 1000$ ft). In contrast to the AEDT contours, which are nearly symmetrical about both the x - and y -axes, the AMAT contours are also nearly symmetric about the x -axis, but the contours can be seen to narrow at the beginning of the flight path and widen at the end of the flight path. This is due to the polar directivity included in the

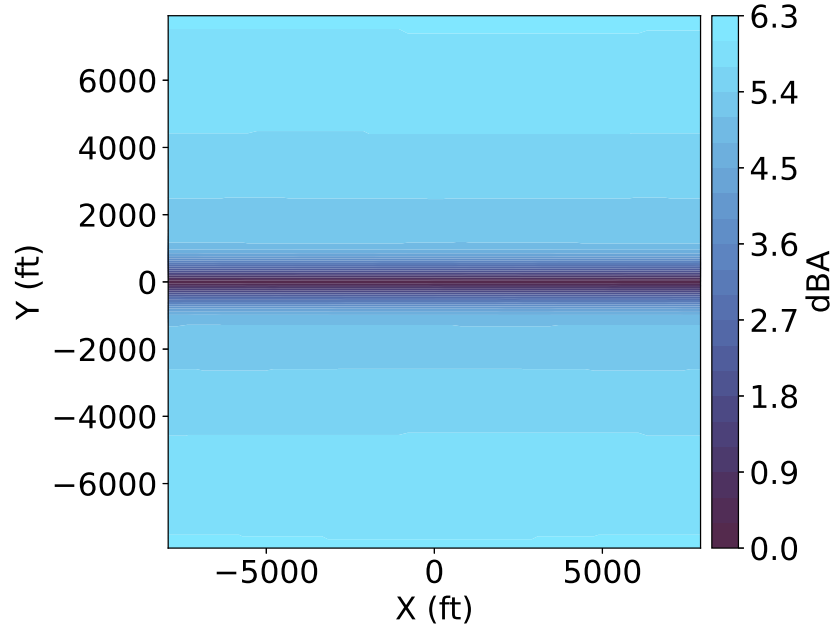


Figure 4: Difference between L_{AE} for fixed-wing and helicopter modes when including lateral directivity.

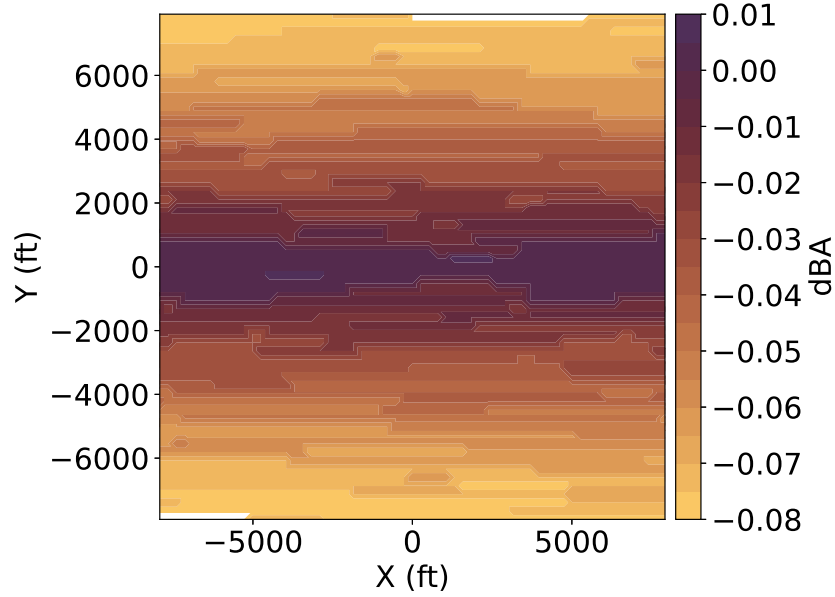


Figure 5: Difference between L_{AE} for fixed-wing and helicopter modes when using axisymmetric helicopter NPD data.

source noise hemispheres used by the AMAT that is not represented in the NPD data used by the AEDT. Additionally, while the extended centerlines are attenuated in the AEDT contours, they show a spike in noise level in the AMAT contours. The

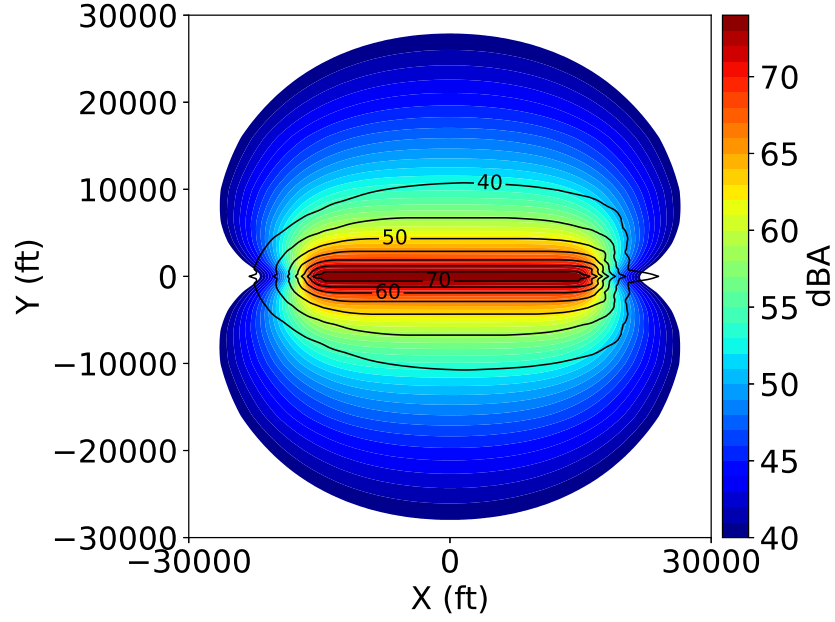


Figure 6: Comparison of AEDT (filled) and AMAT (lines) generated L_{AE} for fixed-wing mode in straight and level overflight.

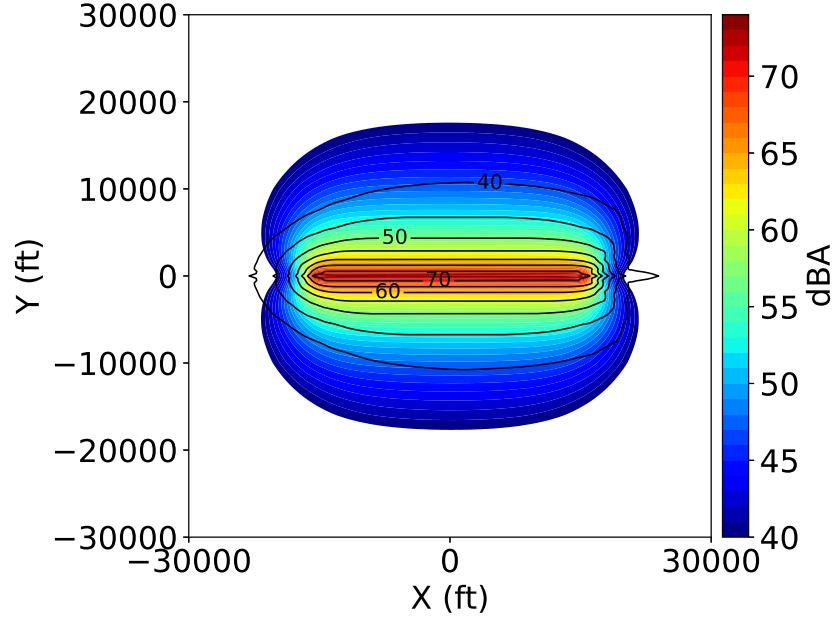


Figure 7: Comparison of AEDT (filled) and AMAT (lines) generated L_{AE} for helicopter mode in straight and level overflight.

latter behavior in the AEDT contours is due to the noise fraction adjustment, and does not appear to have a physical basis according to the AMAT contours.

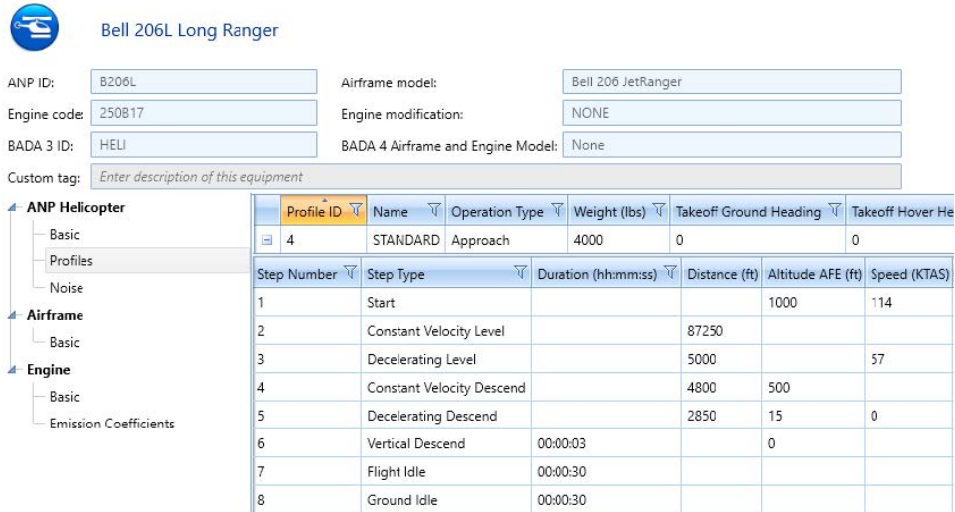
UAM vehicles will fly at lower altitudes relative to fixed-wing aircraft, so com-

munities at angles $> 45^\circ$ may have more significant noise levels relative to typical AEDT-modeled operations. Thus, the relative importance of accurate predictions at higher directivity angles is increased. For azimuthal angles greater than 45° , the outermost fixed-wing AEDT contour level (40 dBA) lies at over double the lateral distance of that shown in the AMAT analysis. As shown by the simulation, the extrapolation used in the AEDT lateral directivity adjustment may not accurately reflect the noise at lateral receptors with azimuthal angles $> 45^\circ$.

3.2 Approach

In Ref. [8], it was shown that for a simple single-segment approach or departure modeled in both fixed-wing and helicopter modes, nearly identical results could be achieved. However, further investigation of more realistic approach and departure profiles is warranted. Also, as shown in Ref. [7], other discrepancies can arise due to the casting process and other helicopter mode restrictions, which are documented in this section.

A nominal approach operation was modeled for the RVLT quadrotor using an adapted version of the standard approach profile of the Bell 206L Long Ranger helicopter in the AEDT ANP database (see Figure 8). This simple profile was selected to permit as comparable an approach operation as possible between the AEDT fixed-wing and helicopter analyses. Figure 9 shows the adapted profile constructed from this basis.



Bell 206L Long Ranger

ANP ID: B206L Airframe model: Bell 206 JetRanger

Engine code: 250817 Engine modification: NONE

BADA 3 ID: HELI BADA 4 Airframe and Engine Model: None

Custom tag: Enter description of this equipment

ANP Helicopter

- Basic
- Profiles
- Noise

Airframe

- Basic

Engine

- Basic
- Emission Coefficients

Profile ID	Name	Operation Type	Weight (lbs)	Takeoff Ground Heading	Takeoff Hover Heading
4	STANDARD	Approach	4000	0	0

Step Number	Step Type	Duration (hh:mm:ss)	Distance (ft)	Altitude AFE (ft)	Speed (KTAS)
1	Start			1000	114
2	Constant Velocity Level		87250		
3	Decelerating Level		5000		57
4	Constant Velocity Descend		4800	500	
5	Decelerating Descend		2850	15	0
6	Vertical Descend	00:00:03		0	
7	Flight Idle	00:00:30			
8	Ground Idle	00:00:30			

Figure 8: Bell 206L Long Ranger standard approach profile used as a basis for the UAM vehicle approach.

Minor changes were required to the standard approach profile including:

- a change in the cruise speed from 114 kt to 90 kt for both fixed-wing and helicopter to match the max speed of the quadrotor reference vehicle.
- correcting the noise exposure data for helicopter mode NPDs to 160 kt (see Section 1.2).

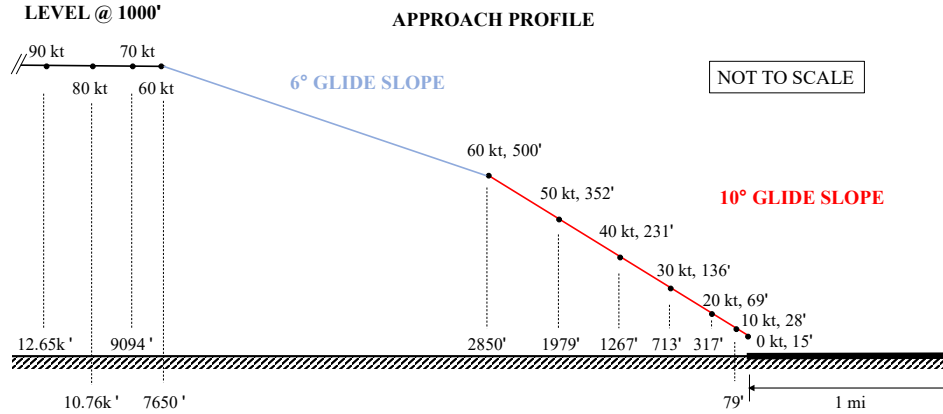


Figure 9: Profile for the AEDT approach analyses. The heavy black horizontal line shows the extent of a one-mile runway with the landing point at the left (west) end. The landing point is located at $(x, y) = 0, 0$ ft, with positive x to the right (east).

- a reduction of the duration of static operational mode procedural steps Y/Z (vertical descent), H (flight idle) and G (ground idle) for helicopter to 0.5 s each to minimize their influence on noise exposure at the landing site. Recall there is no counterpart to these operational mode procedural steps, or I/J (hover) for fixed-wing.
- a reduction of the NPD levels of static operational modes Y/Z (vertical descent), H (flight idle) and G (ground idle) for helicopter to -140 dBA for all metrics. This was because a previous study [8] discovered that despite being only 0.5 s, the inclusion of static modes caused non-negligible differences between the fixed-wing and helicopter contours in the vicinity of the landing area. While this is important to understand and characterize as a difference between fixed-wing and helicopter modeling, it is outside the scope of this current effort.
- adjusting the fixed-wing profile to end at an altitude of 15 ft above field elevation (corresponding to the end of step 5 in Figure 8) to eliminate the need for a precisely vertical descent that is not possible in fixed-wing mode. This was done in conjunction with the previous step to eliminate differences due to the way the end of the profile is handled between fixed-wing and helicopter modes.
- selection of one NPD for helicopter mode A corresponding to the 20 kt, -10° climb angle operating condition. This particular NPD was shown in Figure 23 of Ref. [2] to be in the middle of a range of candidate approach NPDs.
- selection of multiple NPDs for the fixed-wing approach corresponding to the various speeds and climb angles of the profile. This allowed changes to the operating condition as the aircraft decelerated and changed glide angle.

During examination of helicopter NPD data in the ANP database, it was found that:

- Very few helicopters in the database provide L_{Amx} , L_{PNTmx} , or L_{EPN} data for dynamic operational mode procedural steps. Because of the lack of L_{Amx} , this quantity must be computed for use in the noise fraction calculation. Maximum noise level approximation is covered in section 4.2.1.1 of the AEDT 3g Technical Manual [1], where Eq. 4-5 shows how it may be computed as a function of distance and noise exposure. Eq. 4-5 was developed from statistical analysis of NPD data for aircraft containing all four noise metrics in the database. This almost certainly used fixed-wing aircraft data because very few helicopters in the database contain all four noise metrics. Hence, the applicability of Eq. 4-5 to helicopters is in question.
- A comparison was made of AEDT-generated L_{Amx} contours computed using two methods. In one case, the contours were made by specifying both L_{Amx} and L_{AE} NPD data as part of the AEDT input. In the other case, only L_{AE} NPD data were provided as part of the AEDT input. Here, L_{Amx} NPD data were approximated with Eq. 4-5. The L_{Amx} contours generated using the two methods were similar (not shown). Ref. [8] also contains some investigation into the effectiveness of Eq. 4-5 as an approximation tool. It was found that using Eq. 4-5 instead of providing L_{Amx} NPD data for the NASA quadrotor produced differences up to around 2 dBA astride the flight path segment and along the extended centerline. Additionally, up to 4 dBA difference lobes appear astride the extended centerlines.
- Most helicopters provide the minimum of dynamic operational mode procedural steps (A – approach, D – departure, L – level flyover) and static mode procedural steps (G – ground idle or H – flight idle, I – hover in ground effect or J – hover out of ground effect) with other modes provided by substitution with 0 dBA adjustments.

Additionally, since the goal of this section is to compare AEDT fixed-wing approaches with AEDT helicopter approaches, it is necessary that the vehicle (however it is modeled in the AEDT) touches down at the same location. Specifying the touchdown area at a helipad is straightforward; the final approach procedural step always ends at the helipad. When modeling a VTOL aircraft as a fixed-wing aircraft in the AEDT, care must be taken in the specification of displaced thresholds and threshold crossing heights (see AEDT Technical Manual [1] Section 3.6.2.6). A fixed-wing aircraft touches down on the runway at a distance D from the approach end of the runway, per Ref. [1] Eq. 3-34,

$$D = D_{app} + \Delta_{trk} + \frac{h_{tc} \cdot |d_{-1}|}{z_{-1}} \quad (2)$$

in which D_{app} is the displaced approach threshold (ft) for the runway, h_{tc} is the threshold crossing height (ft) for the runway, Δ_{trk} is the delta distance (ft) for the departure ground track and d_{-1} and z_{-1} are the coordinates (ft) and altitude (ft)

of the profile point immediately before touch down. To ‘stick’ the landing of the fixed-wing aircraft at the approach end of the runway co-located with an analogous helipad, it is necessary to set D_{app} and h_{tc} to zero when defining the runway, and Δ_{trk} to zero when defining the track. These are not the default AEDT values.

In the following analyses, the approach end of the runway is located at the same coordinates as the helipad, namely, $x = 0$ ft, $y = 0$ ft. The vehicles are approaching from the negative x -direction.

The bird’s eye views of the L_{AE} contours for the fixed-wing (Figure 10) and helicopter (Figure 11) modes on approach appear quite different from one another. This was also observed in Ref. [6], though the character of the differences is different in the current study due to the 160 kt reference speed workaround for helicopter mode (see Section 1.2). The fixed-wing analysis indicates large lobes to both sides of the landing point, and the helicopter analysis indicates similar side lobes, though with much smaller magnitude. As with the overflight contours (Section 3.1), the bulb-like shape of these contours is attributed to the 4th-power model used in the noise fraction equation, see Ref. [8].

To investigate the differences between these analyses, the fixed-wing analysis is performed using one NPD curve for the initial level flight portion and a different NPD curve for all deceleration and descent segments. The NPD curves correspond to the reference NPD data used for the helicopter mode analyses, e.g., 90 kt, 0° for the level segment and 20 kt, -10° for the descent segments. This makes the input data to the fixed-wing analysis essentially the same as those for the helicopter analysis. (Henceforth, this type of study will be referred to as ‘modified fixed-wing mode’.) The modified fixed-wing analysis is shown in Figure 12. Then, the helicopter is examined without the effects of lateral directivity, that is, replicating the centerline NPD for the right/left NPD at $\phi = \pm 45^\circ$, which is shown in Figure 13. (Recall the axisymmetric study performed in Section 3.1; henceforth, this type of study will be referred to as ‘modified helicopter mode’.) Here, the effect is seen to be a widening of the contours because the centerline NPD data are higher in magnitude than the original $\phi = \pm 45^\circ$ data. The difference between the baseline fixed-wing mode and helicopter mode analyses (Figures 10 and 11) is shown in Figure 14. The difference between the modified fixed-wing approach and the modified helicopter approach (Figures 12 and 13) is shown in Figure 15.

The magnitude of the differences between the baseline studies is fairly large. In particular, there is an area between $x = -7000$ ft and $x = -3000$ ft with differences of up to 12 dBA. This corresponds to the region of 6° descent shown in Figure 9. In this region, the fixed-wing approach is using the 60 kt, -5° climb angle NPD data, and the helicopter approach is using the 20 kt, -10° climb angle NPD data. While it is impossible to say which one is more “correct” at this stage of the analysis, one would certainly infer that the NPD data that more closely resemble the actual operating condition would likely be more representative of the true noise contours.

In contrast, the magnitude of the differences between the modified studies is fairly small. Setting the operating conditions to be nearly the same for the full approach profiles eliminates nearly all differences for $x < 0$. There are some small, but non-negligible differences that extend beyond the approach point, peaking at 2.7 dBA (helicopter greater than fixed-wing, in this case) at around $x = 400$ ft. The

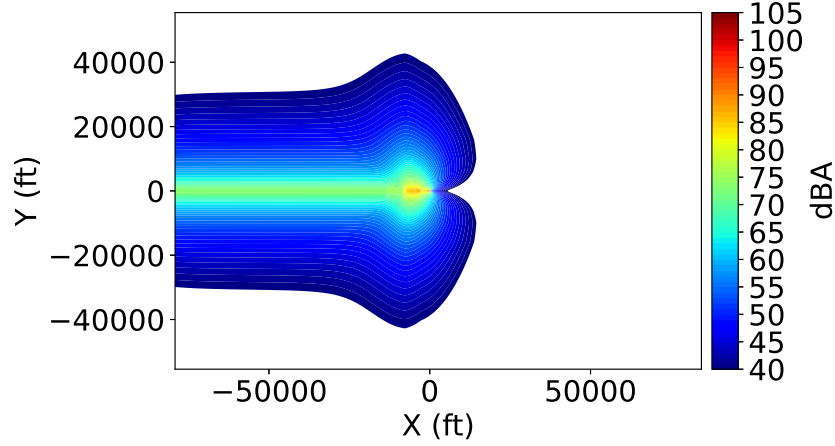


Figure 10: L_{AE} for fixed-wing mode on approach.

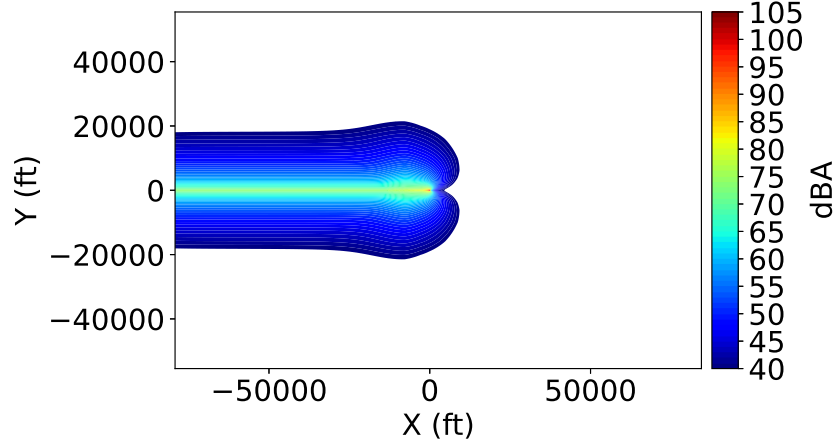


Figure 11: L_{AE} for helicopter mode on approach with lateral directivity.

source of this particular set of differences may warrant further investigation; these differences, however, occur in an area where the predicted noise exposure is under 40 dBA. Thus, the relative importance of these differences is somewhat muted.

It can be concluded the primary sources of the differences between the baseline fixed-wing and helicopter mode analyses shown in Figure 14 are as follows:

- the inclusion of the lateral directivity adjustment LD_{ADJ} for helicopter mode
- the discrepancy between the multiple NPD curves allowed in fixed-wing mode versus the restricted number allowed in helicopter mode

As shown in Figure 15, when steps are taken to neutralize these two parameters, the differences between the analyses become very small.

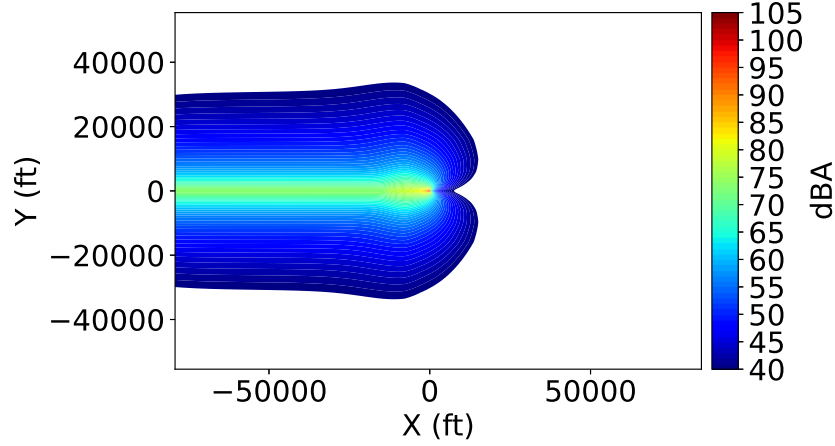


Figure 12: L_{AE} for fixed-wing mode on approach using 2 NPD curves.

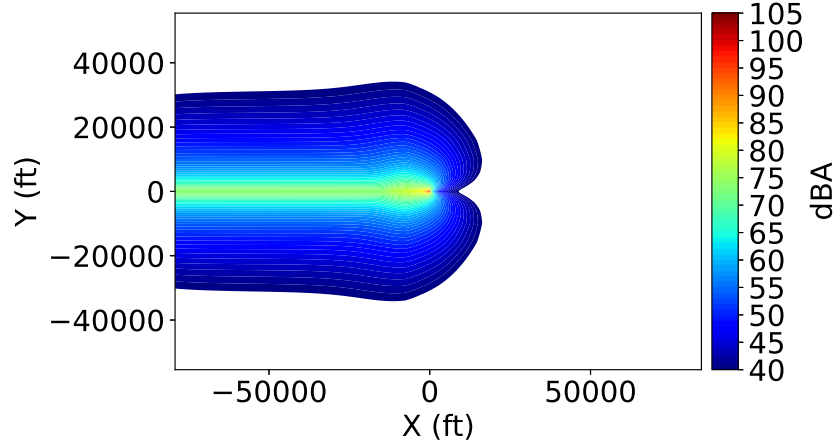


Figure 13: L_{AE} for helicopter mode on approach without lateral directivity.

A Brief Note on Landing and Takeoff Rolls For all receptors beyond the end of the landing roll, a special case of the noise fraction equation (Ref. [1] Eq. 4-24) is applied to the fixed-wing exposure calculation instead of the normal noise fraction equation. This is explored in more detail in Ref. [8]. However, this special case is not relevant to this work. Only an approach ending with a landing roll will invoke the special case, and this must be done deliberately when defining the profile. In procedural mode, a landing roll segment must be specified, and in fixed-point mode, the profile must end with at least two points at 0 ft AFE altitude. None of the profiles in this work, nor those in the larger set of routes studied in Refs. [6] and [9], meet this criterion.

Analogously, there is a special case of the fixed-wing noise fraction calculation for points behind the takeoff roll on departure profiles (Ref. [1] Eq. 4-21). This is

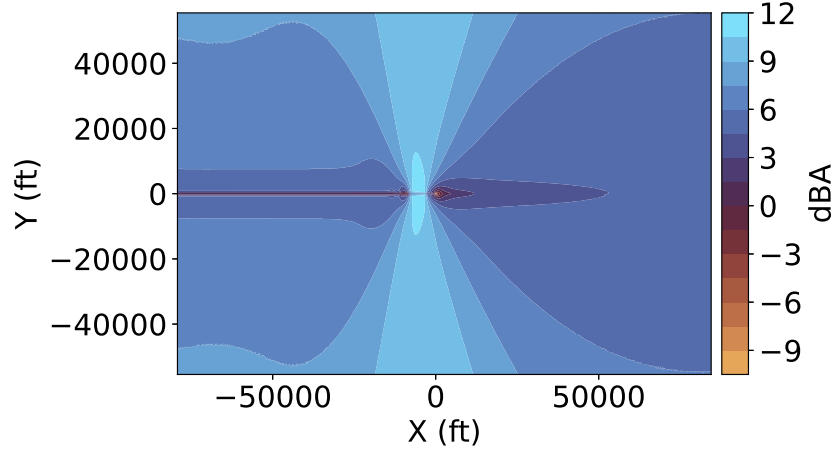


Figure 14: Difference between baseline approach analyses (Figure 10 and Figure 11). Positive difference indicates that the fixed-wing analysis predicts higher noise exposure than the helicopter analysis at that location.

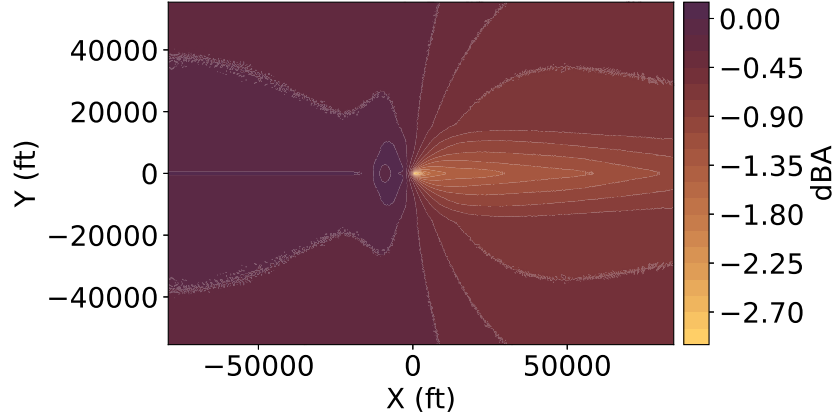


Figure 15: Difference between modified approach analyses (Figure 12 and Figure 13). Positive difference indicates that the fixed-wing analysis predicts higher noise exposure than the helicopter analysis at that location.

only invoked if there is a takeoff roll in the departure profile. In procedural mode, a takeoff roll segment must be specified, and in fixed-point mode, the profile must begin with at least two points at 0 ft AFE altitude. None of the profiles in this or the prior studies [6,9] meet this criterion. This also disables the ground-based directivity adjustment DIR_{ADJ} (Ref. [1] Section 4.4.2).

Both the special case noise fraction equations and DIR_{ADJ} are only applicable to fixed-wing analyses, and have no known use in the AEDT helicopter mode. Therefore, for eliminating differences between the two modes, the above omissions are desirable.

3.2.1 Comparison of AEDT and Simulation Analyses for Approach

Next, simulation data from the AMAT (using the full source directivity) are compared with the AEDT results for fixed-wing (from Figure 10) and helicopter (from Figure 11) analyses for the approach case. The AMAT analyses use the same sequence of operating conditions as those in the AEDT fixed-wing approach, but with the full source noise hemisphere for each condition. The fixed-wing comparisons are shown over the entire domain in Figure 16 and in a close-up in Figure 17. Likewise, the helicopter comparisons are shown in Figure 18 and Figure 19.

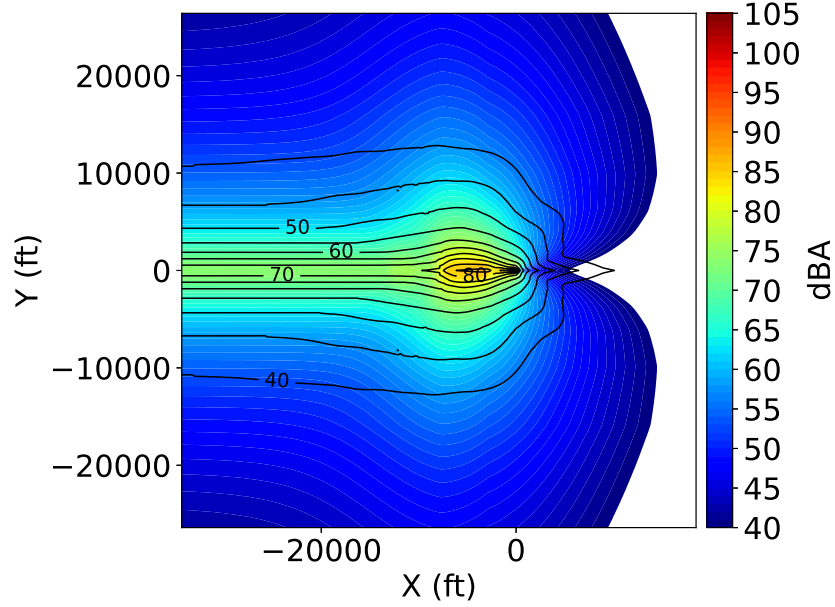


Figure 16: AEDT (filled) and AMAT (lines) L_{AE} contours for fixed-wing mode on approach (full view).

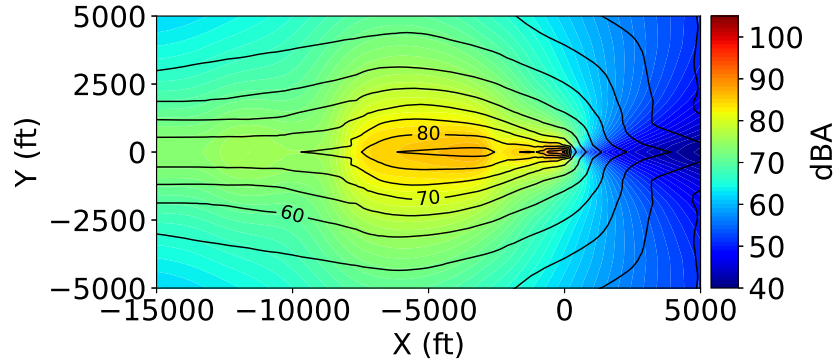


Figure 17: AEDT (filled) and AMAT (lines) L_{AE} contours for fixed-wing mode on approach (close-up view).

As with the overflight case, contour areas under the track compare to the AMAT

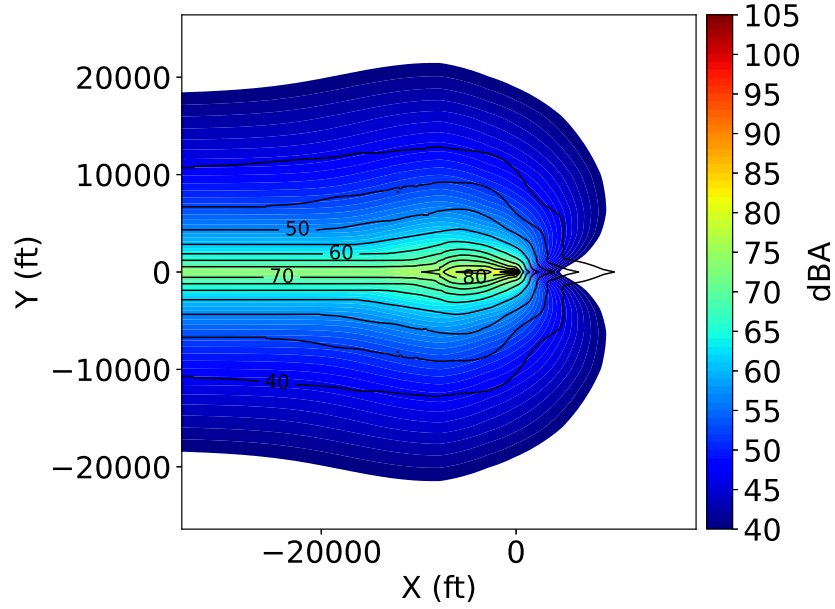


Figure 18: AEDT (filled) and AMAT (lines) L_{AE} contours for helicopter mode on approach (full view).

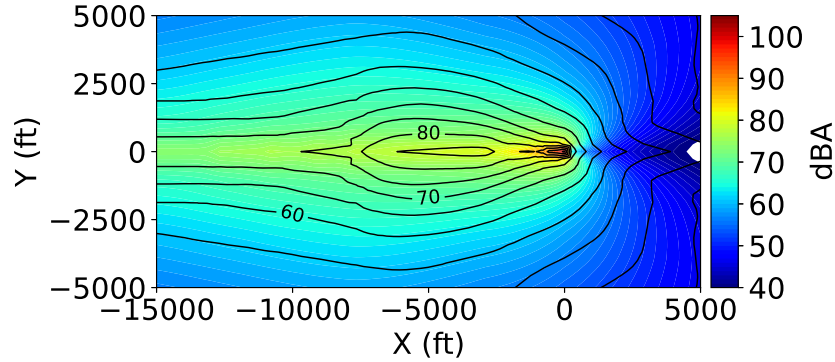


Figure 19: AEDT (filled) and AMAT (lines) L_{AE} contours for helicopter mode on approach (close-up view).

contours favorably for the fixed-wing analysis while those further away do not. This is attributable to the lack of a lateral directivity adjustment for fixed-wing. Close to the landing area, the contours compare quite well, especially for levels $\gtrsim 60$ dBA. One notable difference in character, however, is that the AEDT analysis predicts more attenuation along the extended centerline (along $x > 0, y = 0$), while the AMAT analysis does not. Rather, it predicts the opposite, a small relative increase in levels along the extended centerline compared to other radials from the end of approach point.

In contrast, the comparisons to the AMAT contours for the helicopter mode analysis are much better astride the flight path (the sidelines), but are not as good

along the centerline. Like the overflight case, the contour areas on the level flight segment (preceding the descent), compare more favorably than the fixed-wing case because of the inclusion of the lateral directivity adjustment. However, because the analysis is limited to just a single NPD for approach, the helicopter contours entirely miss the higher-level area along the centerline preceding the landing site. (Recall from Figure 14 the area of elevated differences.)

3.3 Departure

As with the approach analysis, a departure operation was modeled for the RVLTL quadrotor using an adapted version of the standard departure profile of the Bell 206L Long Ranger helicopter in the AEDT ANP database (see Figure 20). This simple profile was selected to permit as comparable a departure operation as possible between AEDT fixed-wing and helicopter analyses. Figure 21 shows the adapted profile constructed from this basis.

Profile ID	Name	Operation Type	Weight (lbs)	Takeoff Ground Heading	Takeoff Hover
4	STANDARD	Approach	4000	0	0
5	STANDARD	Departure	4000	0	0

Step Number	Step Type	Duration (hh:mm:ss)	Distance (ft)	Altitude AFE (ft)	Speed (KTAS)
1	Ground Idle	00:00:30			
2	Flight Idle	00:00:30			
3	Vertical Ascend	00:00:03		15	
4	Accelerating Level		100		30
5	Accelerating Climb		500	30	57
6	Constant Velocity Climb		3500	1000	
7	Accelerating Level		2800		114
8	Constant Velocity Level		93100		

Figure 20: Bell 206L Long Ranger standard departure profile used as a basis for the UAM vehicle departure.

Minor changes were required to the standard departure profile including -

- a change in the cruise speed from 114 kt to 90 kt for both fixed-wing and helicopter to match the max speed of the quadrotor reference vehicle.
- correcting the noise exposure data for helicopter mode NPDs to 160 kt (see Section 1.2).
- a reduction of the duration of static operational mode procedural steps V/W (vertical ascent), H (flight idle) and G (ground idle) for helicopter to 0.5 s each to minimize their influence on noise exposure at the landing site. Recall there is no counterpart to these operational mode procedural steps, or I/J (hover) for fixed-wing.

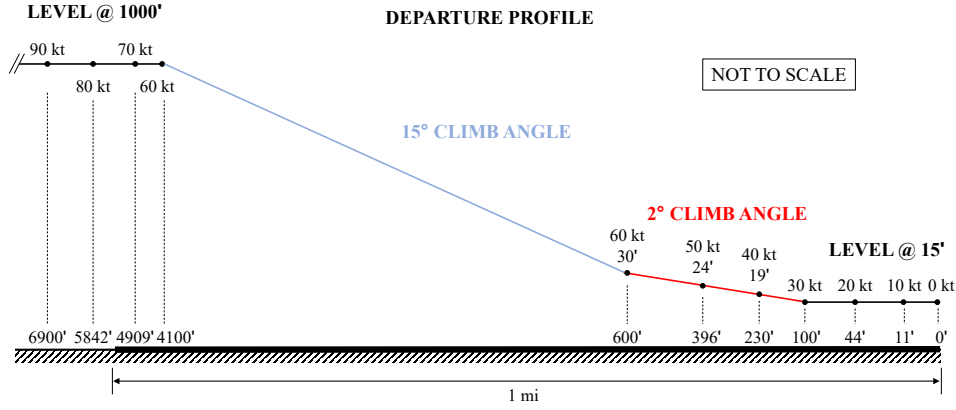


Figure 21: Profile for the AEDT departure analyses. The heavy black horizontal line shows the extent of a one-mile runway with the takeoff point at the right (east) end. The takeoff point is located at $(x, y) = 0, 0$ ft, with positive x to the right (east).

- a reduction of the NPD levels of static operational modes V/W (vertical ascent), H (flight idle) and G (ground idle) for helicopter to -140 dBA for all metrics. (See Section 3.2)
- adjusting the fixed-wing profile to start at an altitude of 15 ft above field elevation (corresponding to the end of step 3 in Figure 20) to eliminate the need for a precisely vertical ascent that is not possible in fixed-wing mode. This was done in conjunction with the previous adjustment to helicopter static mode NPD data to eliminate differences due to the way the start of the profile is handled between fixed-wing and helicopter modes.
- selection of one NPD for helicopter mode D corresponding to the 20 kt, 10° climb angle operating condition. This particular NPD was shown in Figure 21 of Ref. [2] to be in the middle of a range of candidate departure NPDs.
- selection of multiple NPDs for the fixed-wing departure corresponding to the various speeds and climb angles of the profile. This allowed changes to the operating condition as the aircraft accelerated and changed climb angle.

Additionally, since the goal of this section is to compare AEDT fixed-wing departures with AEDT helicopter departures, it is necessary that the vehicle (however it is modeled in the AEDT) takes off from the same location. Specifying the take-off point at a helipad is straightforward; the first departure procedural step always starts at the helipad. As with the approach, care must be taken when modeling a VTOL aircraft as a fixed-wing aircraft for an AEDT departure. A fixed-wing aircraft departure starts at a distance D from the departure end of the runway, per Ref. [1] Eq. 3-33,

$$D = D_{dep} + \Delta_{trk} \quad (3)$$

in which D_{dep} is the displaced departure threshold (ft) for the runway and Δ_{trk} is the delta distance (ft) for the departure ground track. For fixed-wing aircraft to take off from the same location as a helipad located at the departure end of the runway, it is necessary to set D_{dep} to zero when defining the runway and Δ_{trk} to zero when defining the track. These are not the default AEDT values.

In the following analyses, the departure end of the runway is located at the same coordinates as the helipad, namely, $x = 0$ ft, $y = 0$ ft. The vehicles are departing towards the negative x -direction.

The bird’s eye views of the L_{AE} contours for the fixed-wing (Figure 22) and helicopter (Figure 23) modes on departure appear fairly different from one another, but to a lesser extent than the approach. The fixed-wing analysis indicates moderate lobes to both sides of the takeoff point, smaller than those of the approach. The helicopter analysis does not indicate the characteristic side lobes. In Ref. [8], it was shown that the noise fraction adjustments for conjugate approaches and departures (identical flight paths and NPD data, but traveling in reciprocal directions along the flight path) were identical. Therefore, the different character of the departure contours from those of the approach contours shown in Figures 10 and 11 is due to the fact that the departure and approach profiles used in the current study are similar, but not conjugates.

To investigate the differences between these analyses, the modified fixed-wing mode and modified helicopter mode analyses described in Section 3.2 are replicated. The modified fixed-wing departure (two NPDs) is shown in Figure 24, and the modified helicopter departure (axisymmetric) is shown in Figure 25. The difference between the baseline fixed-wing mode and helicopter mode analyses (Figures 22 and 23) is shown in Figure 26. The difference between the modified fixed-wing departure and the modified helicopter departure (Figures 24 and 25) is shown in Figure 27.

Again, the effect of the modified helicopter departure is seen to be a widening of the contours because the centerline NPD data are higher in magnitude than the original $\phi = \pm 45^\circ$ data.

The magnitude of the differences between the baseline studies is fairly large. In particular, there is an area between $x = -4500$ ft and $x = -6500$ ft with differences of up to 10 dBA. This corresponds to the region of horizontal acceleration shown in Figure 21. In this region, the fixed-wing departure is using the 60-80 kt, 0° climb angle NPD data, and the helicopter approach is using the 20 kt, 10° climb angle NPD data. While it is impossible to say which one is more “correct” at this stage of the analysis, one would certainly infer that the NPD data that more closely resemble the actual operating condition would likely be more representative of the true noise contours.

In contrast, the magnitude of the differences between the modified studies is fairly small. Setting the operating conditions to be nearly the same for the full departure profiles eliminates nearly all differences for $x < 0$. There are some small, but non-negligible differences that extend behind the takeoff point, peaking at 1.3 dBA (helicopter greater than fixed-wing, in this case). Notably, at the takeoff point $x = 0, y = 0$, the fixed-wing exposure is 3 dB greater than the helicopter exposure. This is due to a difference in the way helicopter and fixed-wing profiles are formulated, i.e., the fixed-wing profile is flown at the average speed between

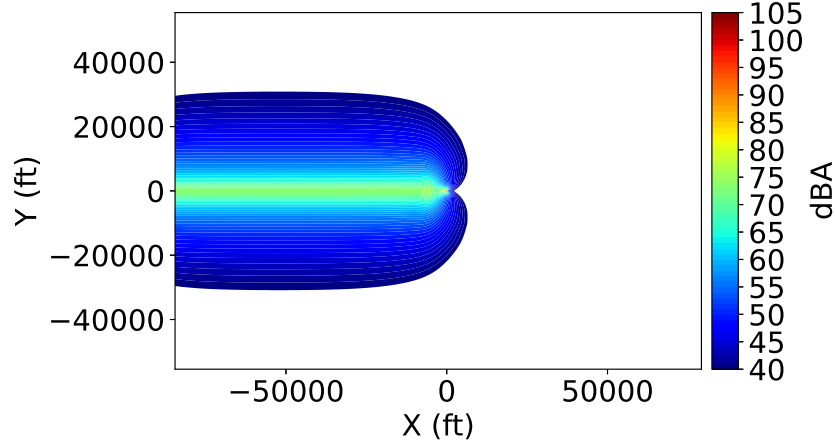


Figure 22: L_{AE} for fixed-wing mode on departure.

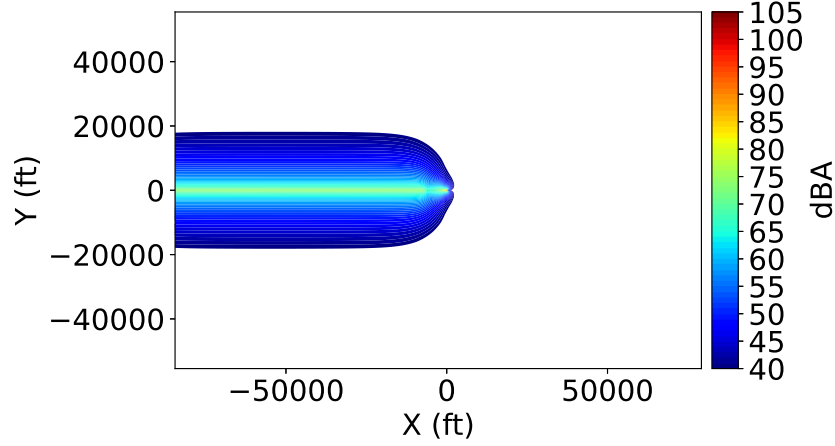


Figure 23: L_{AE} for helicopter mode on departure with lateral directivity.

the segment end points, which results in its speed being half that of the helicopter profile for this segment. This causes a 3 dB difference in the duration adjustment. Outside of this one point, the differences occur in an area where the predicted noise exposure is under 40 dBA. Thus, the relative importance of these differences is somewhat muted.

3.3.1 Comparison of AEDT and Simulation Analyses for Departure

Next, simulation data from the AMAT (using the full source directivity) are compared with the AEDT results for the fixed-wing (from Figure 22) and helicopter (from Figure 23) analyses. The AMAT analyses use the same sequence of operating conditions as those in the AEDT fixed-wing departure, but with the full source noise hemisphere for each condition. The fixed-wing comparisons are shown over the entire domain in Figure 28 and in a close-up in Figure 29. Likewise, the helicopter

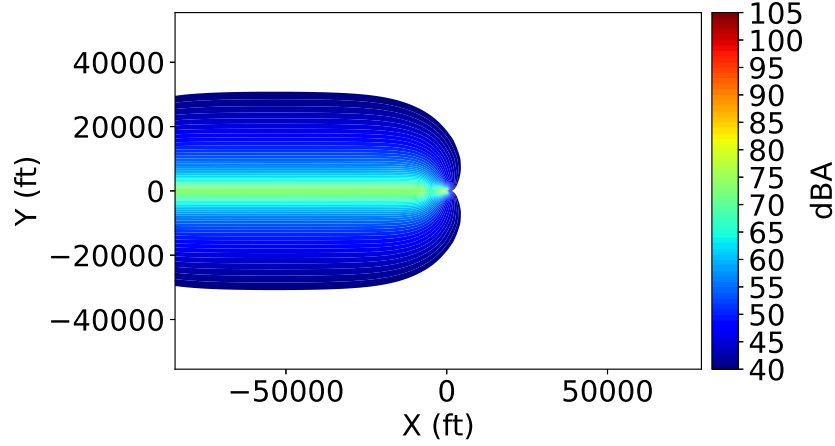


Figure 24: L_{AE} for fixed-wing mode on departure using 2 NPD curves.

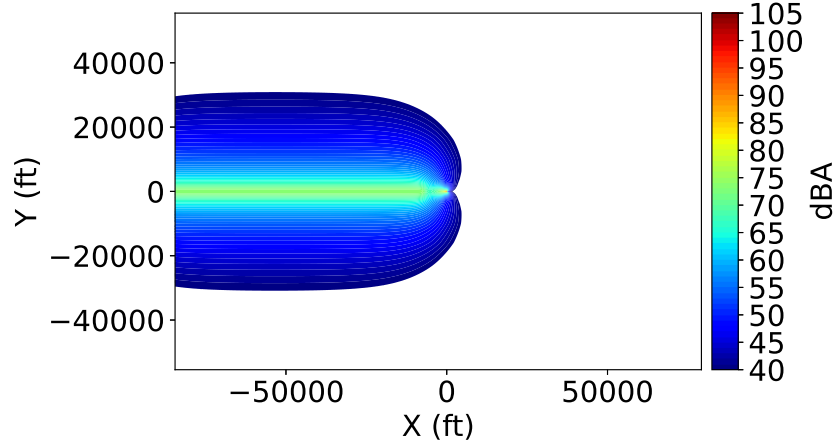


Figure 25: L_{AE} for helicopter mode on departure without lateral directivity.

comparisons are shown in Figure 30 and Figure 31.

As with the overflight case, contour areas under the track compare favorably with the fixed-wing analysis while those further away do not. This is attributable to the lack of a lateral directivity adjustment for fixed-wing. Close to the takeoff area, the contours compare quite well, especially for levels $\gtrsim 60$ dBA. As with the approach, one notable difference in character is that the AEDT analysis predicts more attenuation along the extended centerline (along $x > 0, y = 0$), see Figure 29. The AMAT analysis does not predict this trend; rather, it predicts the opposite, a small relative increase in levels along the extended centerline compared to other radials from the beginning of departure point.

In contrast, the comparisons to the AMAT contours for the helicopter mode are much better astride the flight path (the sidelines) but are not as good along the

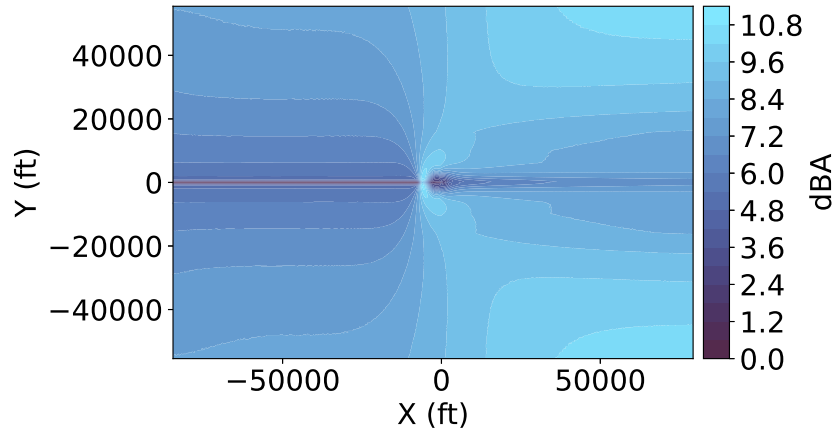


Figure 26: Difference between baseline departure analyses (Figure 22 and Figure 23). Positive difference indicates that the fixed-wing analysis predicts higher noise exposure than the helicopter analysis at that location.

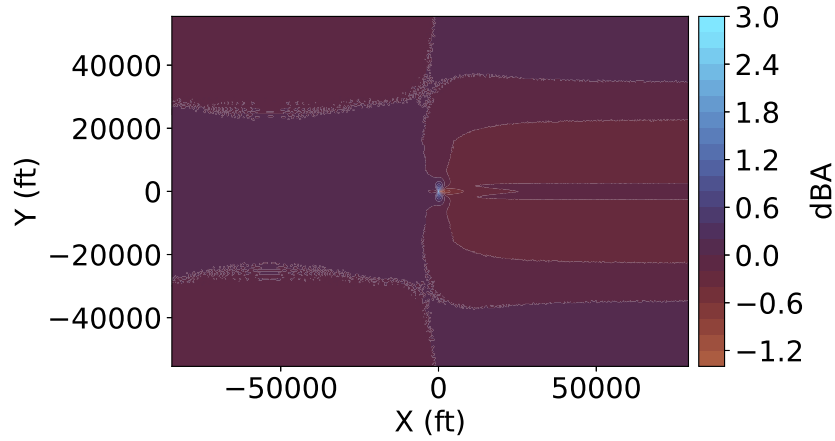


Figure 27: Difference between baseline departure analyses (Figure 24 and Figure 25). Positive difference indicates that the fixed-wing analysis predicts higher noise exposure than the helicopter analysis at that location.

centerline. Like the overflight case, the contour areas on the level flight segment (following the ascent) compare more favorably than the fixed-wing case because of the inclusion of the lateral directivity adjustment. However, because the analyses are limited to just a single NPD for departure, the helicopter contours miss an area of slightly elevated level shortly after takeoff (around $x = -6000$ ft).

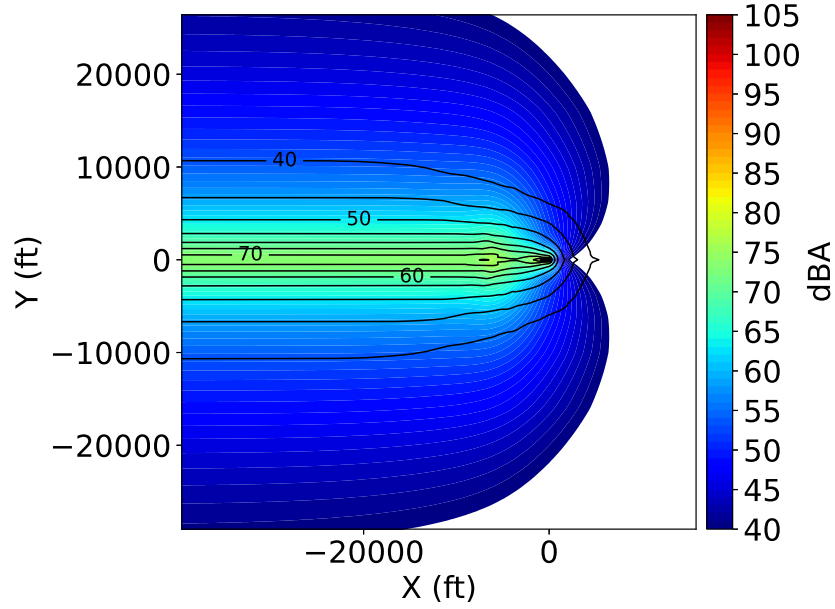


Figure 28: AEDT (filled) and AMAT (lines) generated L_{AE} for fixed-wing mode on departure (full view).

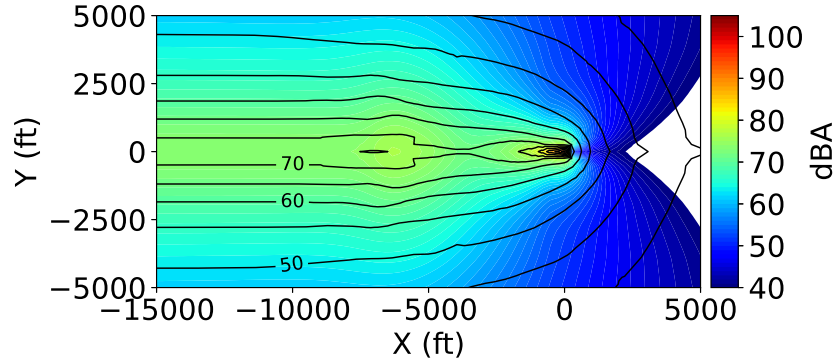


Figure 29: AEDT (filled) and AMAT (lines) generated L_{AE} for fixed-wing mode on departure (close-up view).

4 Recommendations

This final set of recommendations for changes to the AEDT 3g to better support the noise modeling of AAM operations includes those preliminary recommendations made in 2023 (where applicable) and new/updated recommendations.

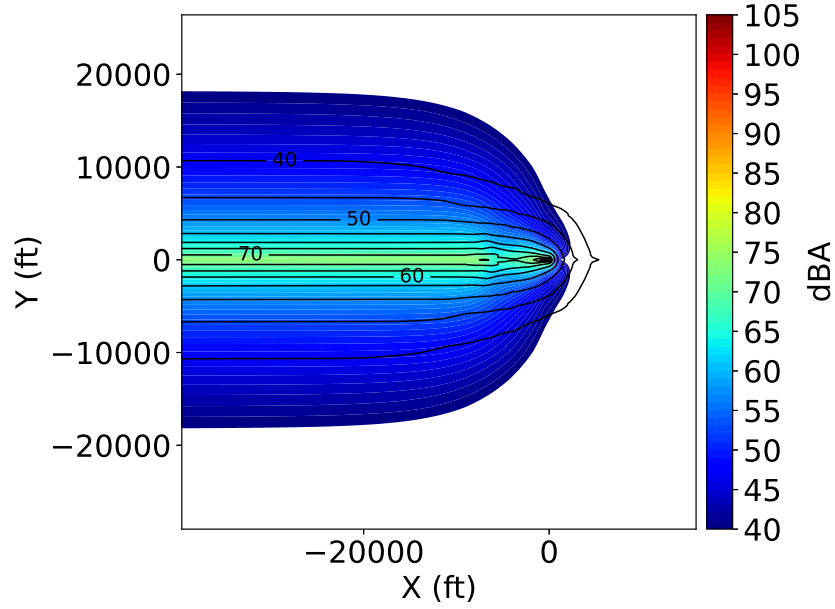


Figure 30: AEDT (filled) and AMAT (lines) generated L_{AE} for helicopter mode on departure (full view).

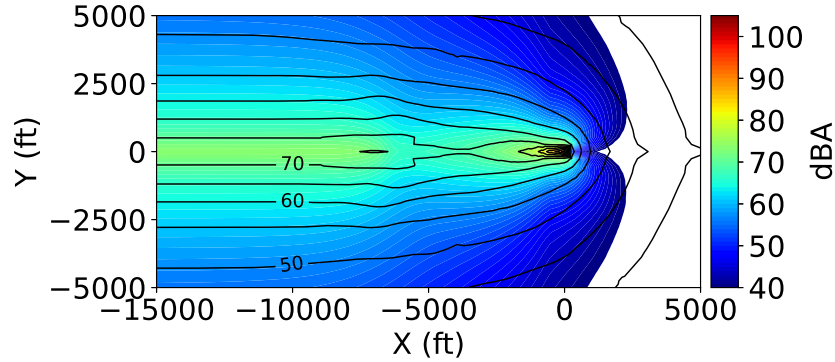


Figure 31: AEDT (filled) and AMAT (lines) generated L_{AE} for helicopter mode on departure (close-up view).

4.1 Fixed-Wing Modeling

4.1.1 Prior Recommendations

- Provide the means of turning off interpolation over corrected net thrust. This would eliminate the necessity to specify guard points to limit the bad effects of interpolation (abrupt contour discontinuities and non-consecutive thrust indexing leading to unintended interpolation) between two dissimilar operating conditions, each with different noise characteristics [9].
- Provide a lateral directivity adjustment (LD_{ADJ}) akin to that for helicopters

(or better) to allow for improved modeling lateral to the ground track.

- Add a hover capability that captures the vehicle source directivity without application of the noise fraction algorithm (as in helicopter mode).

4.1.2 New Recommendations

- For comparison of fixed-wing and helicopter mode departures and approaches, some additional guidance in the AEDT User Manual would be helpful to force the takeoff and landing locations to be the same (see Sections 3.2 and 3.3).
- It was unclear from the documentation that a “takeoff” and “landing” must be specifically defined for fixed-point profiles by starting or ending the profile with two points at zero altitude. This should be made more clear, particularly in the sections about the special case noise fraction and takeoff roll directivity adjustment.

4.2 Helicopter Modeling

4.2.1 Prior Recommendations

- Increase the number of operational modes and associated noise data (including NPD and spectral class).
 - These should be user-defined to allow for modes that don’t presently exist, e.g., decelerating climb.
 - This would eliminate the need for use of the advancing tip Mach number adjustment (which may not be applicable) to condense multiple level flight operations into a single level flight step.
- Eliminate many/all of the restrictions on the sequence of operational procedural steps. The only one that appears useful is that the current step begins where the prior step left off.
- The “in-ground effect” altitude should be user-specified and not hard-coded to 1.5x main rotor diameter (AEDT Technical Manual Eq. 3-74 [1]).

Though not an AEDT recommendation, a standard along the lines of SAE AIR-1845A is needed for helicopter mode NPD generation (see reference in Ref. [2]). Some things to consider include:

- User-defined reference distance (currently set to 200 ft) for the static directivity adjustment. This was examined in Ref. [2].
- Cone angle used for hover condition measurement.

4.2.2 New Recommendations

- The AEDT Technical Manual points out that helicopters use different reference speeds, but it does not point out that these are applied to the different operational mode procedural steps, not the operation type (overflight, departure, or approach). Some clarification of this would be helpful (see Section 3.1).
- If multiple operational mode procedure steps of the same type are allowed in some future version of the AEDT, then either:
 - there will be a need to specify a different reference speed for each change in operational mode procedural step, or
 - follow the fixed-wing process and adjust all helicopter NPD data to a single reference speed, e.g., 160 kt. This is likely the least ambiguous to the provider of helicopter mode NPD data (see Section 3.1).
- Based on the findings in Ref. [8], it may be appropriate to make other power models of the noise fraction available for use. The noise fraction algorithm relies in part on empirical evidence derived from jet aircraft many decades ago. It is unlikely that modern jet aircraft, helicopters and proposed UAM vehicles, many with radically different configurations and power plants, are consistent with this approach. Evidence suggests that the fourth-power model currently used is only marginally applicable to helicopters and AAM vehicles, and that differs between departure, overflight, and approach flight conditions.
- The extrapolation used in the AEDT lateral directivity adjustment may not accurately reflect the noise at lateral receptors with azimuthal angles $> 45^\circ$ (Section 3.1). This will be particularly important for AAM vehicles that fly at low altitudes because noise exposure could be significant for larger azimuthal angles.
- Very few helicopters in the database provide L_{Amx} , L_{PNTmx} , or L_{EPN} data for dynamic operational mode procedural steps. Because of the lack of L_{Amx} , this quantity must be computed for use in the noise fraction calculation. The AEDT maximum noise level approximation is almost certainly based on fixed-wing aircraft data and, as shown in Ref. [8], causes moderate differences in the predicted noise relative to simulated and measured helicopter data.

4.3 Other

4.3.1 Prior Recommendations

- Provide a simple means of specifying point-to-point operations and computer program(s) to simplify study construction.
- Provide support for a single reference elevation for a set of point-to-point operations. With such support, the need to specify overflight altitudes in terms of MSL and departure and approach altitudes in terms of AFE is eliminated.

They can all be altitudes cast in terms of that Above Reference Elevation (ARE).

- The current limitation on spectral classes (departure, overflight, approach) should be removed.
- Expand the lateral directivity adjustment beyond the current left-center-right for helicopter mode and fixed-wing mode (if implemented as recommended above).

4.3.2 New Recommendations

- If no changes are made to the AEDT and the required NPD data are available, then (based on the cases considered):
 - Use of the helicopter aircraft type is recommended for overflight operations because the lateral directivity adjustment more accurately models the noise exposure for receptors lateral to the track.
 - Use of the fixed-wing aircraft type with fixed-point flight profiles is recommended for departure and approach operations because i) there is no restriction on the number of NPD states (allowing changes in operating state to be more accurately reflected), and ii) it provides noise exposure contours that more closely agree with simulation for levels of interest (e.g., sound exposure level > 60 dBA).
 - For point-to-point operations, the above implies a hybrid modeling approach [10] (see also Ref. [6]).

References

1. Aviation Environmental Design Tool (AEDT) Technical Manual, Version 3g. DOT-VNTSC-FAA-24-08, U.S. Department of Transportation, Volpe National Transportation Systems Center, Cambridge, MA, Aug. 2024.
2. Rizzi, S. A.; Letica, S. J.; Boyd, D. D.; and Lopes, L. V.: Prediction of noise-power-distance data for urban air mobility vehicles. *AIAA Journal of Aircraft*, vol. 61, no. 1, Jan. 2024, pp. 166–182. 10.2514/1.C037435.
3. Silva, C.; Johnson, W. R.; Solis, E.; Patterson, M. D.; and Antcliff, K. R.: VTOL urban air mobility concept vehicles for technology development. *2018 Aviation Technology, Integration, and Operations Conference*, June 2018. 10.2514/6.2018-3847.
4. Lopes, L. V.; and Burley, C. L.: ANOPP2 User’s Manual: Version 1.2. Technical Memorandum TM-2016-219342, NASA, Oct. 2016.
5. Volpe Center: Advanced Acoustic Model. Online. URL <https://www.volpe.dot.gov/AAM>.

6. Rizzi, S. A.; and Rafaelof, M.: On the modeling of UAM aircraft community noise in AEDT helicopter mode. *AIAA AVIATION 2023 Forum*, June 2023. 10.2514/6.2023-3363.
7. Letica, S.; and Rizzi, S.: On the modeling of urban air mobility vehicle take-off and landing operations in the FAA Aviation Environmental Design Tool. *INTER-NOISE and NOISE-CON Congress and Conference Proceedings*, vol. 269, July 2024, pp. 270–282. 10.3397/nc_2024_0035.
8. Rizzi, S. A.; and Letica, S. J.: Exposition of noise fraction adjustments for integrated noise modeling of rotary-wing vehicles. *AIAA AVIATION 2025 Forum*, July 2025. 10.2514/6.2025-3413.
9. Rizzi, S. A.; and Rafaelof, M.: Community noise assessment of urban air mobility vehicle operations using the FAA Aviation Environmental Design Tool. *INTER-NOISE and NOISE-CON Congress and Conference Proceedings*, vol. 263, Aug. 2021, pp. 450–461. 10.3397/IN-2021-1482.
10. Noise modeling methods for urban air mobility vehicles in the Federal Aviation Administration’s Aviation Environmental Design Tool. DOT-VNTSC-NASA-22-02, U.S. Department of Transportation, Volpe National Transportation Systems Center, Cambridge, MA, Sept. 2022.